FIFTH ORDER WEIGHTED POWER-ENO METHODS FOR HAMILTON-JACOBI EQUATIONS

SUSANA SERNA* AND JIANLIANG QIAN†

Abstract. We design a class of Weighted Power-ENO (Essentially Non Oscillatory) schemes to approximate the viscosity solution of Hamilton-Jacobi equations. The essential idea of the Power-ENO scheme is to apply an extended class of limiters to the classical third order ENO schemes to improve algorithmic behaviors near discontinuities. Then a weighting strategy based on appropriate smoothness indicators lifts the accuracy of schemes to fifth order accuracy. Numerical experiments demonstrate accuracy and robustness of the new schemes.

Key words. Hamilton-Jacobi, ENO, Weighted Power-ENO, level set, monotone schemes

1. Introduction. We consider the initial value problem for the Hamilton Jacobi equation

$$\phi_t + H(x, \phi, \nabla\phi) = 0, \quad \phi(x,0) = \phi_0(x), \ x \in R^d, \ t > 0, \tag{1.1}$$

where H is a non-decreasing function of ϕ.

Such Hamilton-Jacobi (HJ) equations appear in many applications, for example, geometrical optics, optimal control, differential games, material sciences and calculus of variations. Therefore, it is essential to develop efficient, high order accurate numerical methods to solve such equations.

Theoretically, the generalized weak solution, so-called viscosity solution, exists, is unique and depends on the initial data continuously [7, 2, 5]. Computationally, such a viscosity solution can be approximated by monotone schemes [8, 5]. Since monotone schemes are at most first order accurate for approximating viscosity solutions, a lot of efforts were devoted to designing efficient, highly accurate numerical schemes for such equations; see [16, 17, 9, 1, 12, 14, 2, 22, 3, 6, 4, 18] and references therein. In this paper we design a class of new schemes for such equations based on Weighted

*Departamento de Matematica Aplicada, University of Valencia, Spain. Research supported by DGICYT project BFM2001-2814. Email: **susana.serna@uv.es**

†Department of Mathematics, UCLA, Los Angeles, CA 90095-1555. Research supported by ONR Grant #N00014-02-1-0720. Email: **qian@math.ucla.edu**

Power-ENO ("Essentially Non-Oscillatory") schemes, which is formally fifth order accurate.

The ENO schemes were originally proposed for hyperbolic conservation laws by Harten, Engquist, Osher and Chakravathy [11]. Later the schemes were adapted to solve Hamilton-Jacobi equations by Osher and Sethian [16], and Osher and Shu [17]. Liu, Osher and Chan [15] proposed the Weighted ENO schemes to overcome some shortcomings of ENO schemes, such as poor parallelizability. Afterwards, Jiang and Shu [13] realized that the weighting strategy may yield other advantages besides parallelizability, such as high order accuracy and stability. Moreover, Jiang and Peng [12] extended such strategy to design WENO schemes for Hamilton-Jacobi equations. Since then, such weighting strategy has been used successfully in designing high order schemes for Hamilton-Jacobi equations: Weighted central ENO schemes [3], Hermite WENO schemes [18], high order WENO schemes on unstructured meshes [22]. In this work we propose yet another weighted method for Hamilton-Jacobi equations, the so-called Weighted Power-ENO schemes.

The Weighted Power-ENO schemes were originally developed by Serna and Marquina [19] for hyperbolic conservation laws. The essential idea of the Power-ENO scheme is to apply an extended class of limiters on second order differences to the classical third order ENO schemes to improve algorithmic behaviors near discontinuities. Then a weighting strategy based on appropriate smoothness indicators [13] improves the accuracy of the scheme to fifth order accuracy. Since there exist some well known relations between HJ equations and conservation laws, we adapt such Weighted PowerENO schemes to HJ equations. But since HJ equations are not conservative, we are also able to design a new scheme specifically for HJ equations, and this scheme is not appropriate for conservation laws. Comparing to the standard WENO fifth order scheme, the resulting scheme enjoys similar overhead and has much better capability of resolving viscosity solutions to higher order accuracy.

The paper is organized as follows. In Section 2, we present some monotone schemes and derive Weighted Power-ENO schemes. In Section 3, we give extensive numerical examples to demonstrate the accuracy of the new schemes. We conclude the paper in Section 4.

2. Numerical Schemes.

2.1. Monotone Schemes. We restrict our discussion to the two-dimensional case of problem (1.1):

$$\phi_t + H(x, y, \phi, \phi_x, \phi_y) = 0, \;\; \phi(x, y, 0) = \phi_0(x, y), \;\; t > 0. \tag{2.1}$$

Let (x_j, y_k, t^n) be a uniform discretization of $R^2 \times [0, T]$ with mesh sizes $\Delta x, \;\Delta y$ and Δt. $\phi^n_{j,k}$ denotes a numerical approximation to the viscosity solution of equation (2.1),

$$\phi(x_j, y_k, t^n) = \phi(j\Delta x, k\Delta y, n\Delta t). \tag{2.2}$$

In the following displays the dependence on x, y and ϕ has been suppressed for the sake of clarity. We consider a first order monotone scheme,

$$\phi^{n+1}_{j,k} = \phi^n_{j,k} - \Delta t\, g\Big(\frac{\Delta^x_- \phi^n_{j,k}}{\Delta x}, \frac{\Delta^x_+ \phi^n_{j,k}}{\Delta x}, \frac{\Delta^y_- \phi^n_{j,k}}{\Delta y}, \frac{\Delta^y_+ \phi^n_{j,k}}{\Delta y}\Big), \tag{2.3}$$

where g is a Lipschitz continuous, consistent and monotone flux. Here consistency with H means that $g(u, u, v, v) = H(u, v)$, and monotonicity of g means that g is non increasing in its second and fourth arguments and non decreasing in the other two;

$$\Delta^x_- \phi^n_{j,k} = \phi^n_{j,k} - \phi^n_{j-1,k}; \;\; \Delta^x_+ \phi^n_{j,k} = \phi^n_{j+1,k} - \phi^n_{j,k}; \tag{2.4}$$

$$\Delta^y_- \phi^n_{j,k} = \phi^n_{j,k} - \phi^n_{j,k-1} \;\; \Delta^y_+ \phi^n_{j,k} = \phi^n_{j,k+1} - \phi^n_{j,k}\,. \tag{2.5}$$

We use the method of lines to integrate the HJ equation in time with an explicit TVD Runge-Kutta scheme [20, 21]. We may choose different monotone fluxes as the basis for first order schemes [16, 17]. In the numerical examples, we have used the following three monotone fluxes.

The monotone Lax-Friedrichs flux is defined by:

$$g^{LF}(u^-, u^+, v^-, v^+) = H\Big(\frac{u^- + u^+}{2}, \frac{v^- + v^+}{2}\Big) - \frac{1}{2}\alpha_1(u^+ - u^-) - \frac{1}{2}\alpha_2(v^+ - v^-),$$

where, for $a \le u \le b$ and $c \le v \le d$, $\alpha_1 = \max|H_1(u, v)|$ and $\alpha_2 = \max|H_2(u, v)|$, $H_j(u, v)$ being the partial derivative of H with respect to the jth argument.

The Godunov flux reads as follows [17]:

$$g^{G_1}(u^-, u^+, v^-, v^+) = \mathrm{ext}_{v\in I(v^-,v^+)}\ \mathrm{ext}_{v\in I(u^-,u^+)}\ H(u,v),$$

where $I(a,b) = [\min(a,b), \max(a,b)]$, and

$$\mathrm{ext}_{u\in I(a,b)} = \begin{cases} \min_{a\le u\le b} & a \le b, \\ \\ \min_{b\le u\le a} & a > b. \end{cases}$$

When $H(u,v) = h(u^2, v^2)$, such that $h_1 \cdot h_2 > 0$, where h_j is the partial derivative of h with respect to the jth argument, we use the Osher-Sethian flux [16]:

$$g^{G_2}(u^-, u^+, v^-, v^+) = \begin{cases} h([\max((u^-)^+, (u^+)^-)]^2, [\max((v^-)^+, (v^+)^-)]^2) & h_1 \ge 0, \\ \\ h([\max((u^-)^-, (u^+)^+)]^2, [\max((v^-)^-, (v^+)^+)]^2) & otherwise, \end{cases}$$

where $(a)^+ = \max(a, 0)$ and $(a)^- = -\min(a, 0)$.

To obtain formal higher order accuracy for HJ equations, the strategy is to first approximate spatial derivatives with higher order finite differences, insert them into monotone fluxes, and use higher order TVD Runge-Kutta time stepping to march in time.

2.2. Weighted PowerENO Methods. The classical third order ENO scheme on a uniform mesh uses an adaptive procedure to choose one three-point stencil among three three-point candidate stencils. Since such a three-point stencil uniquely determines a parabola, the ENO strategy boils down to using only one parabola among three available parabolas. The Power-ENO was designed by incorporating a new class of limiters into the classical third order ENO schemes. The limiters in the classical ENO schemes are replaced by a class of weaker limiters, so-called the power$_p$ limiters; then the new limiters are applied to neighboring second order differences so that more information of fine scales is retained.

A carefully designed convex combination of the three candidate parabolas gives rise to the Weighted Power-ENO method; the scheme was applied to the hyperbolic conservation laws [19] and demonstrated to have better capability to resolve discontinuities in solution.

To obtain better behavior near discontinuities of the solution gradient, we adapt the Weighted Power-ENO method to tackle the HJ equations. In the following we first describe power limiters; then we detail the fifth order Weighted Power-ENO schemes.

Let $x > 0$ and $y > 0$ be positive numbers. For a natural number p, the power-p mean, $\text{power}_p(x, y)$, was defined in [19]:

$$\text{power}_p(x, y) = \frac{(x + y)}{2} \left(1 - \left|\frac{x - y}{x + y}\right|^p\right). \tag{2.6}$$

It is easy to verify that the following inequalities hold for any $x > 0$ and $y > 0$:

$$\min(x, y) \le \text{power}_p(x, y) \le \text{power}_q(x, y) \le \frac{x + y}{2}$$

when $0 < p < q$. Moreover,

$$\lim_{p\to\infty} \text{power}_p(x, y) = \frac{x + y}{2} := \text{power}_\infty(x, y). \tag{2.7}$$

Since the reconstruction procedure for the multi-dimensional HJ equations that we are going to use is dimension-by-dimension, it suffices to consider the one-dimensional case of the HJ equation

$$\phi_t + H(\phi_x) = 0. \tag{2.8}$$

We first compute forward differences,

$$z_{j+\frac{1}{2}} = \frac{\Delta^x_+ \phi^n_j}{\Delta x}, \tag{2.9}$$

from discrete point values, $\phi = \phi(x_j)$, located at nodes x_j. Next we associate three polynomials with each interval $I_j = [x_j, x_{j+1}]$. We point out that first order approximations of u^+ and u^- at the node x_j are $u^+_j = u^+(x_j) = z_{j+\frac{1}{2}}$ and $u^-_j = u^-(x_j) = z_{j-\frac{1}{2}}$.

Next we introduce the following notation for the differences:

$$d_j = z_{j+\frac{1}{2}} - z_{j-\frac{1}{2}}, \tag{2.10}$$

$$d_{j+\frac{1}{2}} = \frac{d_j + d_{j+1}}{2}, \tag{2.11}$$

$$D_{j+\frac{1}{2}} = d_{j+1} - d_j. \tag{2.12}$$

Then the Weighted PowerENO methods are based on a convex combination of the following three candidate parabolas associated with I_j:

$$p_j^P(x) = z_{j+\frac{1}{2}} - \frac{P_j}{24} + \frac{x - x_{j+\frac{1}{2}}}{\Delta x}\left[d_j + \frac{P_j}{2} + \frac{P_j}{2}\left(\frac{x - x_{j+\frac{1}{2}}}{\Delta x}\right)\right], \tag{2.13}$$

$$p_{j+\frac{1}{2}}(x) = z_{j+\frac{1}{2}} - \frac{D_{j+\frac{1}{2}}}{24} + \frac{x - x_{j+\frac{1}{2}}}{\Delta x}\left[d_{j+\frac{1}{2}} + \frac{D_{j+\frac{1}{2}}}{2}\left(\frac{x - x_{j+\frac{1}{2}}}{\Delta x}\right)\right], \tag{2.14}$$

$$p_{j+1}^P(x) = z_{j+\frac{1}{2}} - \frac{P_{j+1}}{24} + \frac{x - x_{j+\frac{1}{2}}}{\Delta x}\left[d_{j+1} - \frac{P_{j+1}}{2} + \frac{P_{j+1}}{2}\left(\frac{x - x_{j+\frac{1}{2}}}{\Delta x}\right)\right], \tag{2.15}$$

where $P_j := \text{powermod}_p(D_{j-\frac{1}{2}}, D_{j+\frac{1}{2}})$. Here $\text{powermod}_p(x, y) = \frac{(\text{sign}(x)+\text{sign}(y))}{2}\text{power}_p(|x|, |y|)$.

At $x = x_j$, we have

$$p_j^P(x_j) = z_{j+\frac{1}{2}} - \frac{1}{2}d_j - \frac{1}{6}P_j, \tag{2.16}$$

$$p_{j+\frac{1}{2}}(x_j) = z_{j+\frac{1}{2}} - \frac{1}{2}d_{j+\frac{1}{2}} - \frac{1}{6}D_{j+\frac{1}{2}}, \tag{2.17}$$

$$p_{j+1}^P(x_j) = z_{j+\frac{1}{2}} - \frac{1}{2}d_{j+1} + \frac{1}{3}P_{j+1}. \tag{2.18}$$

The convex combination to obtain optimal accuracy for $u^+(x_j)$ at the left interface of I_j is

$$u^+(x_j) = w_0 \cdot p_j^P(x_j) + w_1 \cdot p_{j+\frac{1}{2}}(x_j) + w_2 \cdot p_{j+1}^P(x_j), \tag{2.19}$$

where

$$w_k = \frac{\alpha_k}{\alpha_0 + \alpha_1 + \alpha_2} \tag{2.20}$$

for $k = 0, 1, 2$, and

$$\alpha_k = \frac{C_k}{(\epsilon + IS_k)^2}. \tag{2.21}$$

Here $C_0 = 0.6$, $C_1 = 0.2$ and $C_2 = 0.2$ are the optimal weights, and the smoothness indicators are

$$IS_0 = \frac{13}{12}(P_j)^2 + \frac{1}{4}\left(2z_{j+\frac{1}{2}} - 2z_{j-\frac{1}{2}} + P_j\right)^2, \tag{2.22}$$

$$IS_1 = \frac{13}{12}\left(z_{j-\frac{1}{2}} - 2z_{j+\frac{1}{2}} + z_{j+\frac{3}{2}}\right)^2 + \frac{1}{4}\left(z_{j-\frac{1}{2}} - z_{j+\frac{3}{2}}\right)^2, \tag{2.23}$$

$$IS_2 = \frac{13}{12}\left(P_{j+1}\right)^2 + \frac{1}{4}\left(2z_{j+\frac{3}{2}} - 2z_{j+\frac{1}{2}} - P_{j+1}\right)^2, \tag{2.24}$$

where P is the powereno limiter computed for the two neighboring second-order differences. To obtain the above smoothness indicators, we have used the L^2-norm of the derivatives of the polynomials involved so that the optimal degree of accuracy can be achieved [13].

A similar formula for $u^-(x_j)$ is obtained from the polynomials associated with I_{j-1},

$$u^-(x_j) = w_0 \cdot p^P_{j-1}(x_j) + w_1 \cdot p_{j-\frac{1}{2}}(x_j) + w_2 \cdot p^P_j(x_j) \tag{2.25}$$

with $C_0 = 0.2$, $C_1 = 0.2$ and $C_2 = 0.6$ taken as the optimal weights in the formulas (2.20) and (2.21).

In particular, the three parabolas evaluated at the right interface of I_{j-1} are,

$$p^P_{j-1}(x_j) = z_{j-\frac{1}{2}} + \frac{1}{2}d_{j-1} + \frac{1}{3}P_{j-1}, \tag{2.26}$$

$$p_{j-\frac{1}{2}}(x_j) = z_{j-\frac{1}{2}} + \frac{1}{2}d_{j-\frac{1}{2}} + \frac{1}{12}D_{j-\frac{1}{2}}, \tag{2.27}$$

$$p^P_j(x_j) = z_{j-\frac{1}{2}} + \frac{1}{2}d_j - \frac{1}{6}P_j. \tag{2.28}$$

The resulting method is a fifth order accurate Weighted Power ENO method for $p \geq 3$ as shown in [19]. The optimal value of p to get fifth order accuracy for the approximation of hyperbolic conservation laws is $p = 3$ as shown in [19]. Since HJ equations are non conservative and their solutions do not develop jump discontinuities, we are able to design a new scheme specifically for HJ equations and such a scheme is not appropriate for conservation laws. To this end we use the weakest possible limiter in the power limiter class, that is, the Power$_\infty$ mean, to define the Weighted Power$_\infty$ ENO method.

Moreover, simpler expressions for the three parabolas in terms of z_j's are obtained when the Power$_\infty$ mean is invoked:

$$p^P_{j-1}(x_j) = \frac{1}{6}z_{j-\frac{5}{2}} - \frac{2}{3}z_{j-\frac{3}{2}} + \frac{4}{3}z_{j-\frac{1}{2}} + \frac{1}{6}z_{j+\frac{1}{2}},$$

$$p_{j-\frac{1}{2}}(x_j) = -\frac{1}{6}z_{j-\frac{3}{2}} + \frac{5}{6}z_{j-\frac{1}{2}} + \frac{1}{3}z_{j+\frac{1}{2}},$$
$$p_j^P(x_j) = -\frac{1}{12}z_{j-\frac{3}{2}} + \frac{7}{12}z_{j-\frac{1}{2}} + \frac{7}{12}z_{j+\frac{1}{2}} - \frac{1}{12}z_{j+\frac{3}{2}}.$$

In this case, the corresponding smoothness indicators are,

$$IS_0 = \frac{13}{48}\left(z_{j-\frac{5}{2}} - z_{j-\frac{3}{2}} - z_{j-\frac{1}{2}} + z_{j+\frac{1}{2}}\right)^2 + \frac{1}{4}\left(\frac{1}{2}z_{j-\frac{5}{2}} - \frac{5}{2}z_{j-\frac{3}{2}} + \frac{3}{2}z_{j-\frac{1}{2}} + \frac{1}{2}z_{j+\frac{1}{2}}\right)^2,$$

$$IS_1 = \frac{13}{12}\left(z_{j-\frac{1}{2}} - 2z_{j+\frac{1}{2}} + z_{j+\frac{3}{2}}\right)^2 + \frac{1}{4}\left(z_{j-\frac{1}{2}} - z_{j+\frac{3}{2}}\right)^2,$$

$$IS_2 = \frac{13}{48}\left(z_{j-\frac{3}{2}} - z_{j-\frac{1}{2}} - z_{j+\frac{1}{2}} + z_{j+\frac{3}{2}}\right)^2 + \frac{1}{4}\left(\frac{1}{2}z_{j-\frac{3}{2}} - \frac{5}{2}z_{j-\frac{1}{2}} + \frac{3}{2}z_{j+\frac{1}{2}} + \frac{1}{2}z_{j+\frac{3}{2}}\right)^2.$$

The Weighted Power ENO method proposed in [19] is a fifth order accurate reconstruction procedure suitable for the approximation of hyperbolic conservation laws, since it satisfies the "local total variation bounded property (LTVB)", as shown in [19]. This property is important for a reconstruction method to approximate piecewise smooth functions with jump discontinuities.

A limiter is designed to ignore the non-smooth information of discontinuities so that the total variation at jump discontinuities is diminished. However, when the solution is smooth in some region, the limiter also ignores smooth information from neighboring cells such that the loss of accuracy occurs in such smooth regions. Such a drawback is shared by both WENO5 and WPowerENO5 since the coefficients of the convex combination for the three different parabolas may change abruptly, and the resulting method degenerates to third order accuracy. However, the above Weighted Power$_\infty$ ENO method does not suffer from such a drawback because the Power$_\infty$ mean is an arithmetic mean, and the resulting method makes use of smoothness information from neighboring cells. Since it is not LTVB, the Weighted Power$_\infty$ ENO method is not appropriate for the approximation of hyperbolic conservation laws. However, this method is useful for approximation of viscosity solutions to Hamilton-Jacobi equations because viscosity solutions are continuous.

As shown in Theorem 1 of [19], Weighted Power$_\infty$ ENO method is a fifth order accurate method with the smallest local truncation errors among all Weighted Power ENO methods of fifth order accuracy. The main advantage of the WPowerENO is

that it is more centered (local) since the lateral parabolas use information of the central second order difference in contrast to the classical ENO methods that ignore such information. In addition, Weighted Power$_\infty$ ENO is the most centered of all the WPowerENO methods.

3. Numerical experiments. We apply WENO5, Weighted PowerENO5 with p=3, and Weighted Power$_\infty$ENO5 to a set of model problems.

3.1. Example 1. We consider

$$\phi_t + H(\phi_x) = 0,\ -1 \le x \le 1,\ t > 0 \tag{3.1}$$

$$\phi(x,0) = -\cos(\pi x),\ -1 \le x \le 1 \tag{3.2}$$

with a convex flux H, $H(u) = \frac{(u+1)^2}{2}$, and a non-convex flux H, $H(u) = -\cos(u+1)$.

We solve both initial value problems up to two different times $t = t_1 = 0.05$ and $t = t_2 = 0.16$. The solution is smooth up to $t = t_1$, and its derivative is discontinuous at $t = t_2$ in both cases.

In Tables 3.1, 3.2, 3.3 and 3.4, we display the L_∞ and L_1 errors of the schemes under study. At $t = t_2$, the errors are computed at a distance 0.1 away from discontinuities in the derivative of the solution. For time stepping in the three schemes, we have used third order TVD Runge-Kutta schemes [17] by taking $\Delta t \approx \Delta x^{\frac{5}{3}}$ to realize fifth order in time. At t_1 the smallest L_∞-errors are reached by Weighted Power$_\infty$ENO5 method; at t_2 this method has the largest L_∞-errors (due to the presence of discontinuities) among the three methods. We notice that fifth order accuracy in smooth regions is achieved in all the cases.

3.2. Example 2. We solve the linear equation $\phi_t + \phi_x = 0,\ \phi(x,0) = f(x - 0.5)$, $-1 \le x \le 1$ with periodic boundary conditions.

We choose $f(x)$ to be a primitive of the Harten function which is discontinuous [10]:

$$f(x) = -(\frac{\sqrt{3}}{2}+\frac{9}{2}+\frac{2\pi}{3})(x+1)+\begin{cases} 2\cos(\frac{3\pi x^2}{2}) - \sqrt{3}, & -1 \le x \le -\frac{1}{3}; \\ 3/2 + 3\cos(2\pi x), & -\frac{1}{3} \le x \le 0; \\ 15/2 - 3\cos(2\pi x), & 0 \le x \le \frac{1}{3}; \\ (28 + 4\pi + \cos(3\pi x))/3 + 6\pi(x^2 - x), & \frac{1}{3} \le x \le 1. \end{cases}$$

TABLE 3.1
$H(u) = \frac{(u+1)^2}{2}$ *at* $t = 0.05$

Scheme	N	L_∞ error	L_∞ order	L_1 error	L_1 order
WENO-GODUNOV	40	0.16E-04	-	0.50E-04	-
	80	0.76E-06	4.45	0.21E-05	4.59
	160	0.30E-07	4.66	0.88E-07	4.55
WPowerENO-GODUNOV	40	0.56E-04	-	0.76E-04	-
	80	0.20E-05	4.81	0.29E-05	4.70
	160	0.73E-07	4.77	0.11E-06	4.75
WPower$_\infty$ ENO-GODUNOV	40	0.53E-05	-	0.15E-04	-
	80	0.20E-06	4.71	0.60E-06	4.61
	160	0.96E-08	4.39	0.25E-07	4.63

TABLE 3.2
$H(u) = \frac{(u+1)^2}{2}$ *at* $t = 0.16$

Scheme	N	L_∞ error	L_∞ order	L_1 error	L_1 order
WENO-GODUNOV	40	0.31E-03	-	0.38E-03	-
	80	0.86E-05	5.17	0.13E-04	4.87
	160	0.14E-06	5.87	0.26E-06	5.60
	320	0.47E-08	4.96	0.69E-08	5.28
WPowerENO-GODUNOV	40	0.17E-03	-	0.37E-03	-
	80	0.13E-04	3.68	0.25E-04	3.88
	160	0.21E-06	6.04	0.46E-06	5.76
	320	0.22E-08	6.55	0.61E-08	6.24
WPower$_\infty$ENO-GODUNOV	40	0.25E-02	-	0.50E-02	-
	80	0.44E-03	2.52	0.52E-03	3.26
	160	0.24E-04	4.20	0.24E-04	4.41
	320	0.42E-06	5.86	0.43E-06	5.84

The results computed with 100 grid points and CFL= 0.6 at times t=2, 8, 16 and 32 are shown in Figure 3.1. We observe that as time increases all the schemes smooth out the corners. However, both Weighted PowerENO5 and Weighted Power$_\infty$ENO5 methods perform better than the classical WENO5 at the corners in terms of capturing sharp transitions. Moreover, the plots also indicate that the Weighted Power$_\infty$ENO5 method outperforms the other two at those corners.

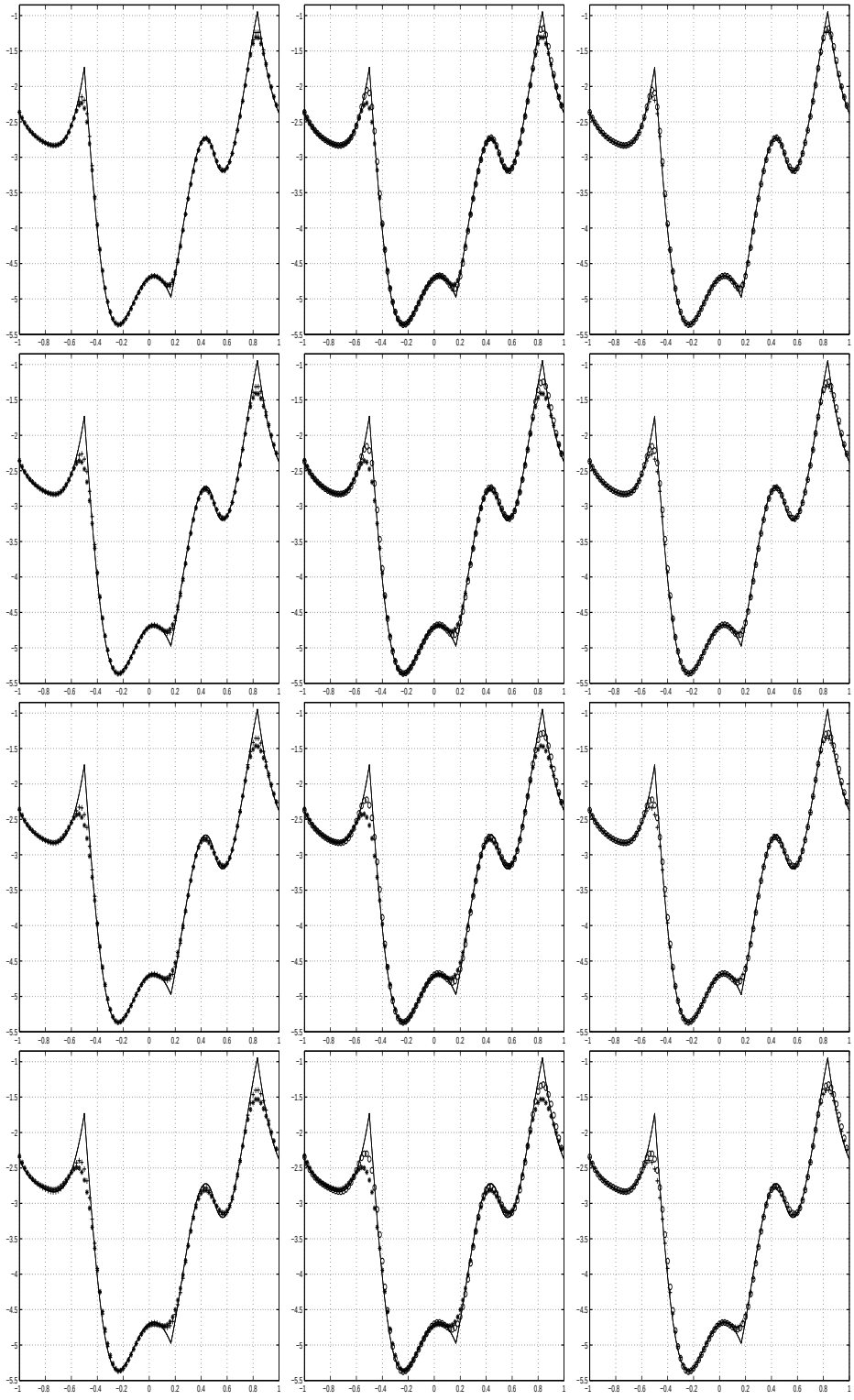

FIG. 3.1. *Comparisons. Left column: WENO5 ('∗') and WPowerENO5 ('+'). Central column: WENO5 ('∗') and W*Power$_\infty$*ENO5 ('o'). Right column: WPowerENO5 ('+') and W*Power$_\infty$*ENO5 ('o').*

TABLE 3.3

$H(u) = -\cos(u+1)$ *at* $t = 0.05$

Scheme	N	L_∞ error	L_∞ order	L_1 error	L_1 order
WENO-GODUNOV	40	0.47E-04	-	0.13E-03	-
	80	0.31E-05	3.89	0.65E-05	4.28
	160	0.14E-06	4.52	0.27E-06	4.60
WPowerENO-GODUNOV	40	0.67E-04	-	0.15E-03	-
	80	0.84E-05	3.05	0.13E-04	3.48
	160	0.73E-06	3.53	0.10E-05	3.73
WPower_∞ ENO-GODUNOV	40	0.30E-04	-	0.99E-04	-
	80	0.21E-05	3.87	0.47E-05	4.41
	160	0.91E-07	4.50	0.19E-06	4.60

TABLE 3.4

$H(u) = -\cos(u+1)$ *at* $t = 0.16$

Scheme	N	L_∞ error	L_∞ order	L_1 error	L_1 order
WENO-GODUNOV	40	0.16E-03	-	0.31E-03	-
	80	0.15E-04	3.41	0.31E-04	3.29
	160	0.71E-06	4.43	0.12E-05	4.76
	320	0.21E-07	5.07	0.35E-07	5.04
WPowerENO-GODUNOV	40	0.12E-03	-	0.28E-03	-
	80	0.11E-04	3.43	0.19E-04	3.88
	160	0.12E-05	3.13	0.13E-05	3.89
	320	0.22E-07	5.78	0.32E-07	5.33
WPower_∞ENO-GODUNOV	40	0.20E-03	-	0.59E-03	-
	80	0.60E-04	1.75	0.70E-04	3.10
	160	0.32E-05	4.24	0.34E-05	4.36
	320	0.44E-07	6.16	0.52E-07	6.03

3.3. Example 3. We solve a 2D nonconvex Riemann problem,

$$\phi_t + \sin(\phi_x + \phi_y) = 0, \quad \phi(x, y, 0) = \pi(|y| - |x|). \tag{3.3}$$

We evolve until time $t = 1$ with a grid of 40×40 points using WENO, WPowerENO and WPower_∞ENO schemes based on the flux g^{G_1}.

All the schemes converge to the viscosity solution. However, there are some differences in the maximum and minimum values reached by the three schemes as

shown in Table 3.5. We observe that the WPower$_\infty$ENO scheme has sharper resolution of discontinuities in derivatives than both WENO and WPowerENO schemes do. We display the results at $t = 1$ in Figure 3.2.

TABLE 3.5

Scheme	maximum	minimum
WENO5	2.3960	-2.4145
WPowerENO	2.4081	-2.4953
WPower$_\infty$ENO	2.8358	-2.6634

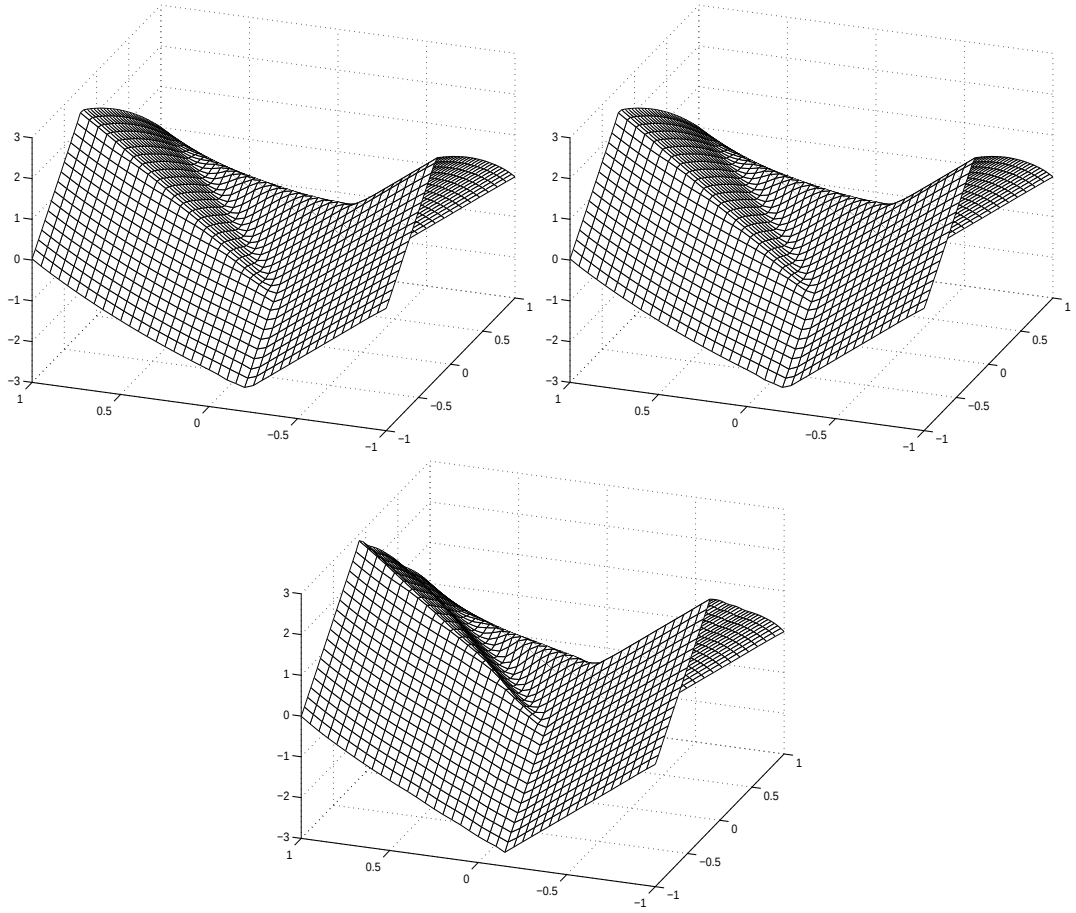

FIG. 3.2. *Top left, WENO. Top right, WPowerENO. Bottom,* WPower$_\infty$*ENO*

3.4. Example 4. We consider a problem related to optimal control [17]:

$$\phi_t - (\sin y)\phi_x + (\sin x + \text{sign}(\phi_y))\phi_y - \frac{1}{2}\sin^2 y - (1 - \cos x) = 0 \tag{3.4}$$

with the initial data $\phi(x, y, 0) = 0$ in the interval $[-\pi, \pi] \times [-\pi, \pi]$. We use a grid of $40\times$ 40 with periodic boundary conditions.

We compute the solution up to t=1 for WENO, WPowerENO and WPower$_\infty$ENO based on the Lax-Friedrichs scheme and the third order TVD Runge-Kutta scheme. We display the results at t=1 in Figure 3.3. We observe that sharper resolution in discontinuities of first derivatives is achieved by WPower$_\infty$ENO.

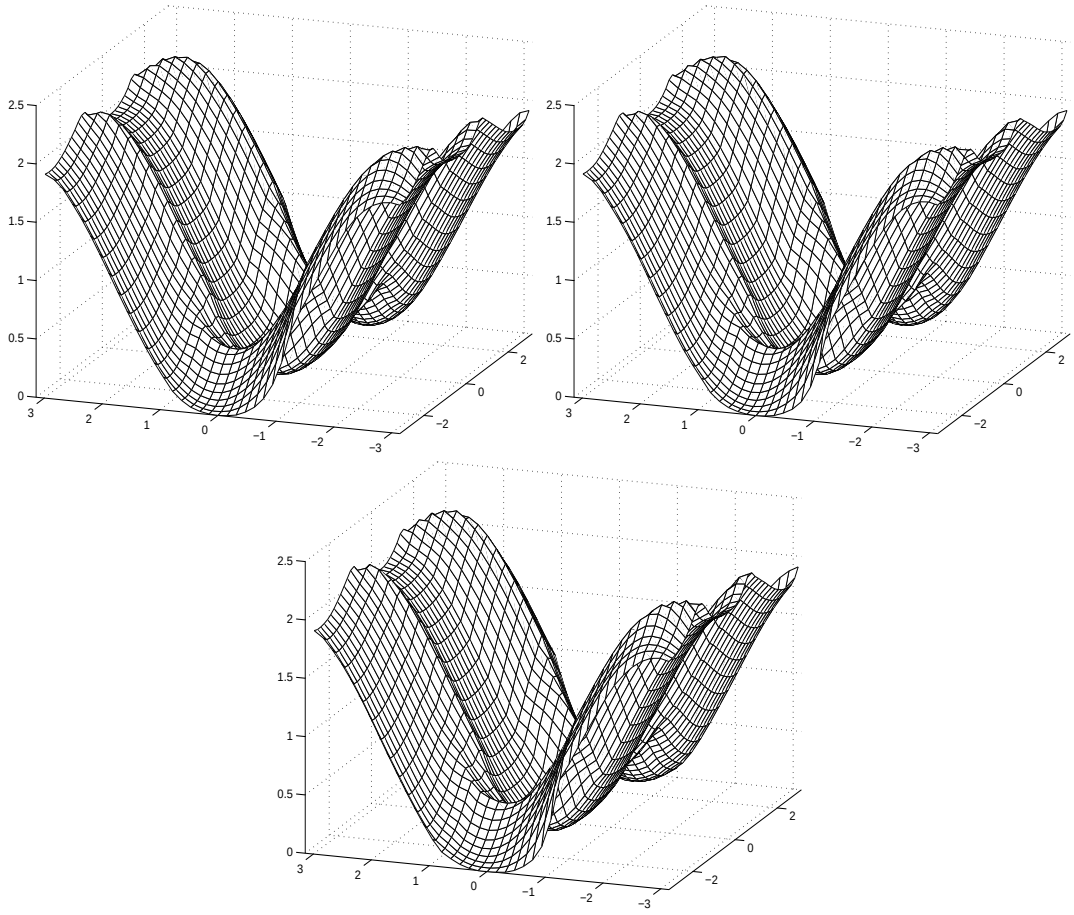

FIG. 3.3. *Top left, WENO. Top right, WPowerENO. Bottom, W*Power$_\infty$*ENO*

3.5. Example 5. Consider the "level set reinitialization" equation

$$\phi_t + \text{sign}(\phi_0)\Big[\sqrt{\phi_x^2 + \phi_y^2} - 1\Big] = 0, \quad \phi(x, y, 0) = \phi_0(x, y). \tag{3.5}$$

We choose ϕ_0 to be the distance function to the circle centered at the origin with radius 1/2, plus some perturbation in radial and angular directions near the circle:

$$\phi_0^1(x,y) = \begin{cases} d+\delta, & |d| \le \epsilon; \\ d, & \text{otherwise;} \end{cases} \tag{3.6}$$

and

$$\phi_0^2(x,y) = \begin{cases} d+2\delta, & |d| \le \epsilon; \\ d, & \text{otherwise,} \end{cases} \tag{3.7}$$

where $d = \sqrt{x^2+y^2} - 0.5$, $\theta = \tan^{-1}(\frac{y}{|x|})$, $\epsilon = 0.2$ and $\delta = \frac{\epsilon}{16\pi}\sin\left(\frac{4\pi d \sin 5\theta}{\epsilon}\right)$. We use $\frac{\phi_0}{\sqrt{\phi_0+(\Delta x)^2}}$ to approximate $\text{sign}(\phi_0)$.

We perform the computation using the Osher-Sethian flux g^{G_2}, which is simpler than the general one g^{G_1}, together with the third order TVD RK stepping in time for the three schemes. We evolve in time using a grid of 100×100 points and a CFL number of 0.6.

We compute ϕ up to different times and compute the mean curvature K, $K \equiv \nabla \cdot \frac{\nabla\phi}{|\nabla\phi|}$ of the level set ϕ contours, by using central differences. As the regularization for the possible zero denominator, we replace $\frac{\nabla\phi}{|\nabla\phi|}$ with $\frac{\nabla\phi}{\sqrt{|\nabla\phi|^2+\Delta x^2}}$.

For the first case corresponding to ϕ_0^1, the maximum of the mean curvature of the initial data is 43.545925 and the minimum is −33.465937; for the second case corresponding to ϕ_0^2, the maximum is 88.5558 and the minimum −66.4770.

Figure 3.4 shows the results for the first case. From top to bottom we display the initial data and the results for steps 16, 64 and 256.

Figure 3.5 shows the results for the second case. From top to bottom we display the initial data and the results for steps 128, 512 and 1024.

From all the three schemes in both cases there are significant differences in the curvature before and after the reinitialization. The curvature computed from the solution of the Weighted Power$_\infty$ENO5 is less noisy in all cases than both the WENO5 and Weighted PowerENO5 methods; the noise persists in some regions for the latter two methods. Although the behaviour of WENO5 and Weighted PowerENO5 is similar, the noise dissipates for the Weighted Power$_\infty$ENO5; we believe that the non-smooth limiters in the WENO5 and Weighted Power ENO methods might cause the

persistence of some degree of noise in the curvature, and the arithmetic mean type limiter in the Weighted Power$_\infty$ENO5 method might be responsible for the better behaviour of the method.

Next, we consider the recovery of a non-smooth distance function. For this purpose, we use ϕ_0 to be the signed distance function, $d_l(x,y)$, to the lemniscate

$$a^4 = [(x-a)^2 + y^2][(x+a)^2 + y^2] \tag{3.8}$$

with $a = 0.5$, plus some perturbation in radial and angular directions near the curve:

$$\phi_0^3(x,y) = \begin{cases} d_l + 3\delta, & |d_l| \le \epsilon, \\ d_l, & \text{otherwise}, \end{cases} \tag{3.9}$$

which is defined in $[-1,1] \times [-1,1]$ with $\delta = \frac{\epsilon}{16\pi} \sin\left(\frac{2\pi d \sin 5\theta}{\epsilon}\right)$, $\epsilon = 0.2$ and $\theta = \tan^{-1}(\frac{y}{|x|})$.

Let us remark that $d_l(x,y)$ has a jump discontinuity in first order partial derivatives along the y-axis.

We evolve in time using a grid of 200×200 and a CFL number of 0.6 for the three schemes. We compute ϕ up to different times and compute the corresponding mean curvature of ϕ in the whole domain excluding a small neighbourhood of the x- and y-axis to improve visualization of the noise in contour lines.

In Figure 3.6, we display the initial perturbed data ϕ_0^3 and the converged solution (to steady state) for the Weighted Power$_\infty$ENO scheme. There is no distinguishable difference in the steady solutions from the three schemes.

Figure 3.7 shows the contour plot of the curvature. From top to bottom we display the initial data and the results for steps 16, 64 and 256.

We remark that the three schemes converge to the steady state very fast and a significant reduction of the noise in the computed curvatures is achieved in all cases.

Finally, we also remark that we have used the fourth order TVD Runge-Kutta time stepping procedure designed by Spiteri and Ruuth [21] in the computation; the main advantage of RK4 is that we can speed up the computation 50% by doubling the CFL number to achieve the same accuracy .

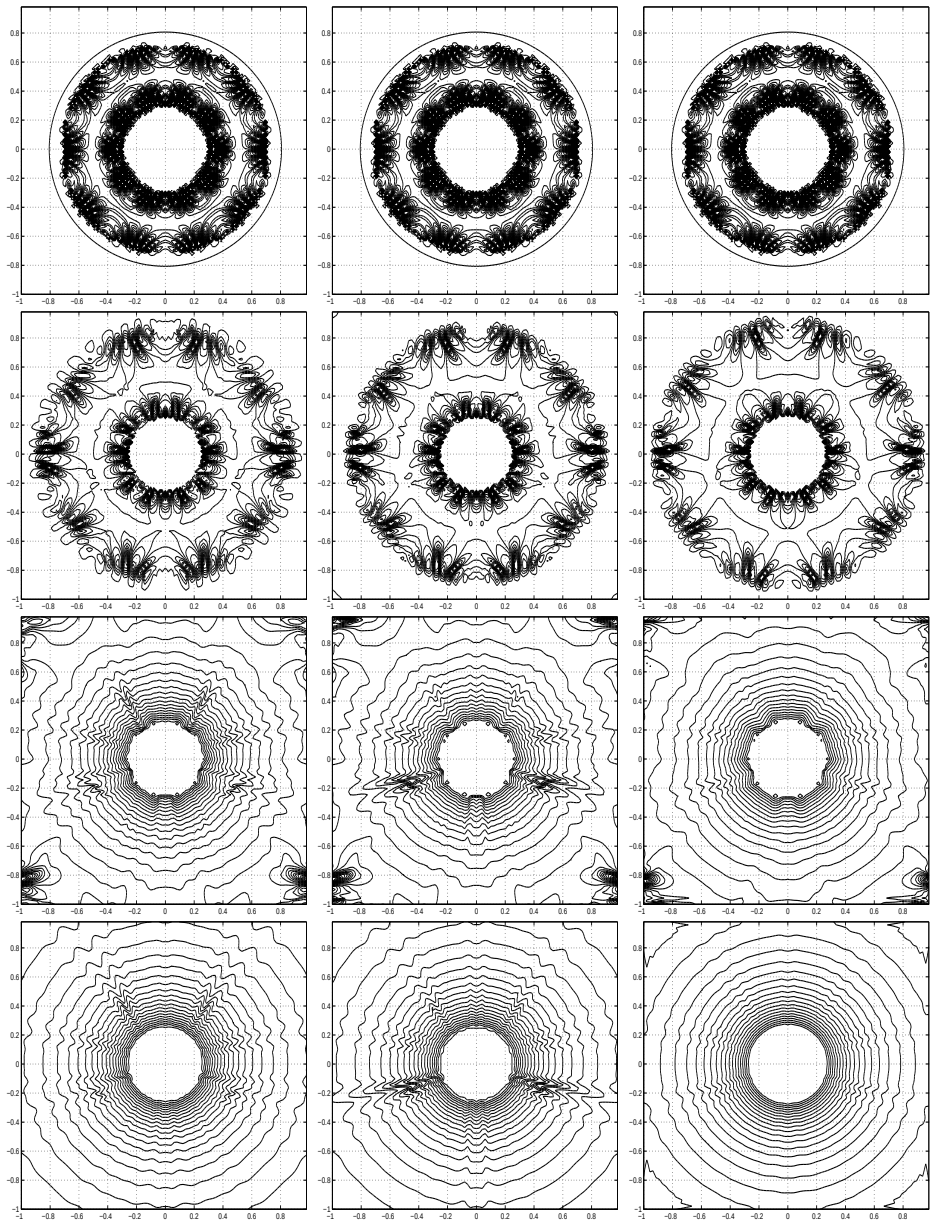

FIG. 3.4. *Curvatures at steps 0, 16, 64, and 256. Left column: WENO. Central column: WPowerENO. Right column: Weighted* Power_∞ *ENO.*

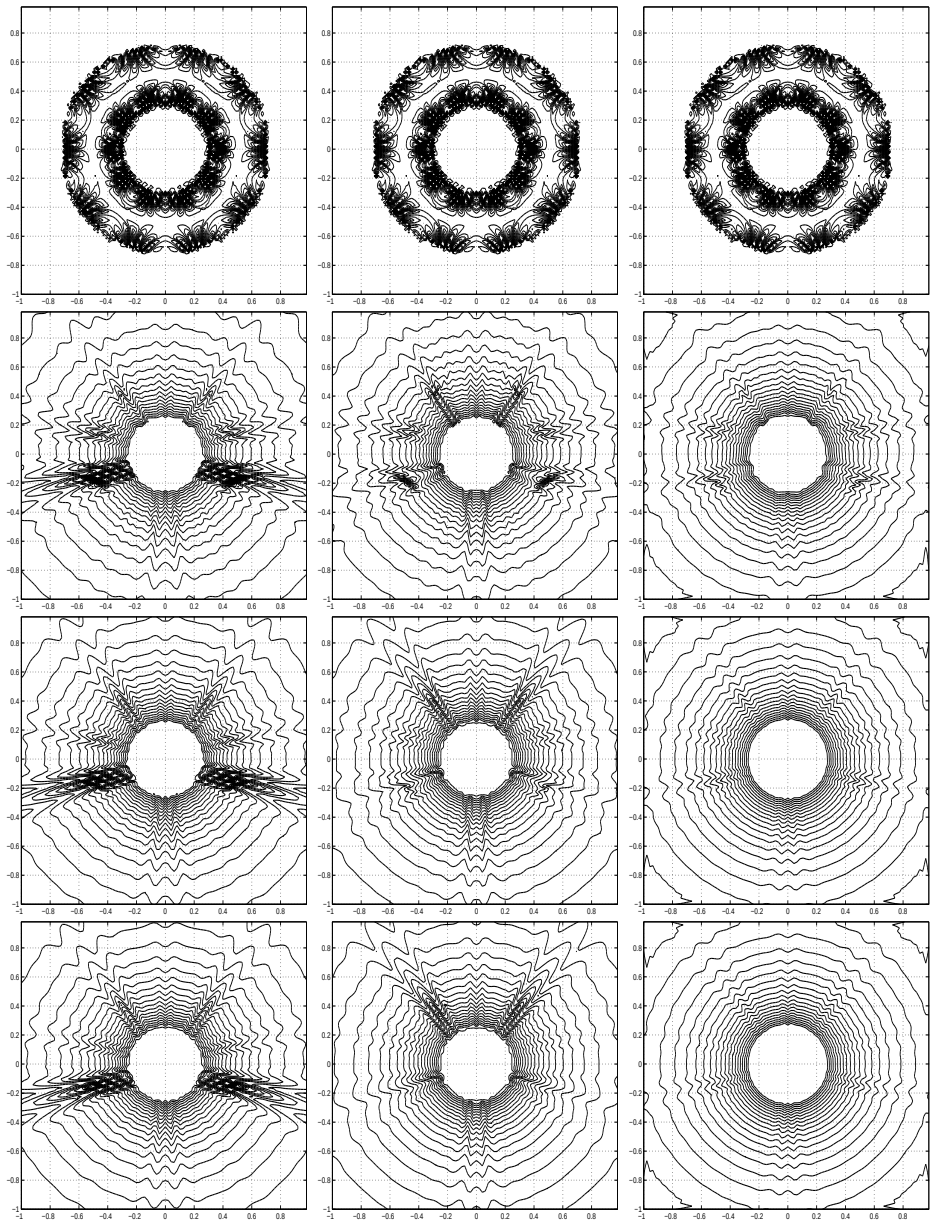

FIG. 3.5. *Curvatures at steps 0, 128, 512 and 1024. Left column: WENO. Central column: WPowerENO. Right column: Weighted* Power_∞ *ENO method.*

4. Conclusion. We have designed a class of Weighted Power-ENO (essentially non oscillatory) schemes to approximate the viscosity solution of the Hamilton-Jacobi equations. The essential idea of the Power-ENO scheme is to apply an extended class of limiters to second order differences in the classical third order ENO schemes to improve algorithmic behaviors near discontinuities. Then a weighting strategy based on appropriate smoothness indicators improves the accuracy of schemes to fifth order accuracy. Numerical experiments have demonstrated accuracy and robustness of the new schemes.

Acknowledgment. The authors would thank Prof. A. Marquina and Prof. S. Osher for discussions on this topic. The first author performed the research reported here while being a guest of the Department of Mathematics at UCLA; Serna thanks the computational and applied mathematics group for its hospitality.

REFERENCES

[1] R. Abgrall. Numerical discretization of the first-order Hamilton-Jacobi equations on triangular meshes. *Comm. Pure Appl. Math.*, 49:1339–1377, 1996.

[2] S. Albert, B. Cockburn, D. French, and T. Peterson. A posteriori error estimates for general numerical methods for Hamilton-Jacobi equations. part I: The steady state case. *Math. Comp.*, 71:49–76, 2002.

[3] S. Bryson and D. Levy. High order central WENO schemes for multi-dimensional Hamilton-Jacobi equations. *SIAM J. Num. Anal.*, 41:1339–1369, 2003.

[4] T. Cecil, J. Qian, and S. J. Osher. High dimensional numerical methods using Radial Basis Functions for Hamilton-Jacobi equations. *J. Comp. Phys.*, 196:327–347, 2004.

[5] B. Cockburn and J. Qian. Continuous dependence results for Hamilton-Jacobi equations. Collected lectures on the preservation of stability under discretization. Edited by D. Estep and S. Tavener. SIAM, Philadelphia, PA, 2002, pp.67-90., 2002.

[6] B. Cockburn and B. Yenikaya. An adaptive method with rigorous error control for the Hamilton-Jacobi equations. part I: the one dimensional steady state case. Preprint, University of Minnesota, 2003.

[7] M. G. Crandall and P. L. Lions. Viscosity solutions of Hamilton-Jacobi equations. *Trans. Amer. Math. Soc.*, 277:1–42, 1983.

[8] M. G. Crandall and P. L. Lions. Two approximations of solutions of Hamilton-Jacobi equations. *Math. Comp.*, 43:1–19, 1984.

[9] M. Falcone and R. Ferretti. Discrete time high-order schemes for viscosity solutions of Hamilton-Jacobi-Bellman equations. *Numer. Math.*, 67:315–344, 1994.

[10] A. Harten. High resolution schemes for hyperbolic conservation laws. *J. Comput. Phys.*, 49:357–393, 1983.

[11] A. Harten, B. Engquist, S. J. Osher, and S. Chakravarthy. Uniformly high order essentially non-oscillatory schemes, III. *J. Comput. Phys.*, 71:231–303, 1987.

[12] G. S. Jiang and D. Peng. Weighted ENO schemes for Hamilton-Jacobi equations. *SIAM J. Sci. Comput.*, 21:2126–2143, 2000.

[13] G. S. Jiang and C. W. Shu. Efficient implementation of weighted ENO schemes. *J. Comput. Phys.*, 126:202–228, 1996.

[14] C. T. Lin and E. Tadmor. High-resolution nonoscillatory central schemes for Hamilton-Jacobi equations. *SIAM J. Sci. Comput.*, 21:2163–2186, 2000.

[15] X. D. Liu, S. J. Osher, and T. Chan. Weighted Essentially NonOscillatory schemes. *J. Comput. Phys.*, 115:200–212, 1994.

[16] S. J. Osher and J. A. Sethian. Fronts propagating with curvature dependent speed: algorithms based on Hamilton-Jacobi formulations. *J. Comput. Phys.*, 79:12–49, 1988.

[17] S. J. Osher and C. W. Shu. High-order Essentially NonOscillatory schemes for Hamilton-Jacobi equations. *SIAM J. Num. Anal.*, 28:907–922, 1991.

[18] J. Qiu and C. W. Shu. Hermite WENO schemes for Hamilton-Jacobi equations. Preprint, Brown University, 2004.

[19] S. Serna and A. Marquina. Power ENO methods: a fifth order accurate weighted Power ENO method. *J. Comput. Phys.*, 194:632–658, 2004.

[20] C. W. Shu and S. J. Osher. Efficient implementation of essentially non-oscillatory shock capturing schemes II. *J. Comput. Phys.*, 83:32–78, 1989.

[21] R. J. Spiteri and S. J. Ruuth. A new class of optimal high order strong stability preserving time discretization methods. *SIAM J. Num. Anal.*, 40:469–491, 2002.

[22] Y.-T. Zhang and C.-W. Shu. High order WENO schemes for Hamilton-Jacobi equations on triangular meshes. *SIAM J. Sci. Comp.*, 24:1005–1030, 2003.

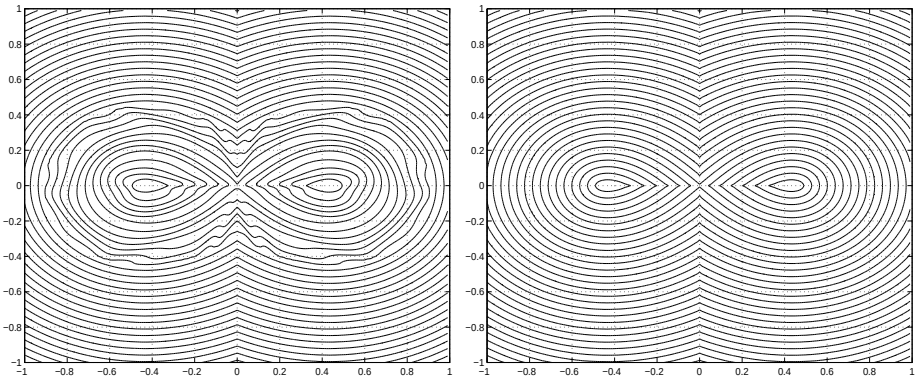

FIG. 3.6. *Left: perturbed initial data. Right: converged solution*

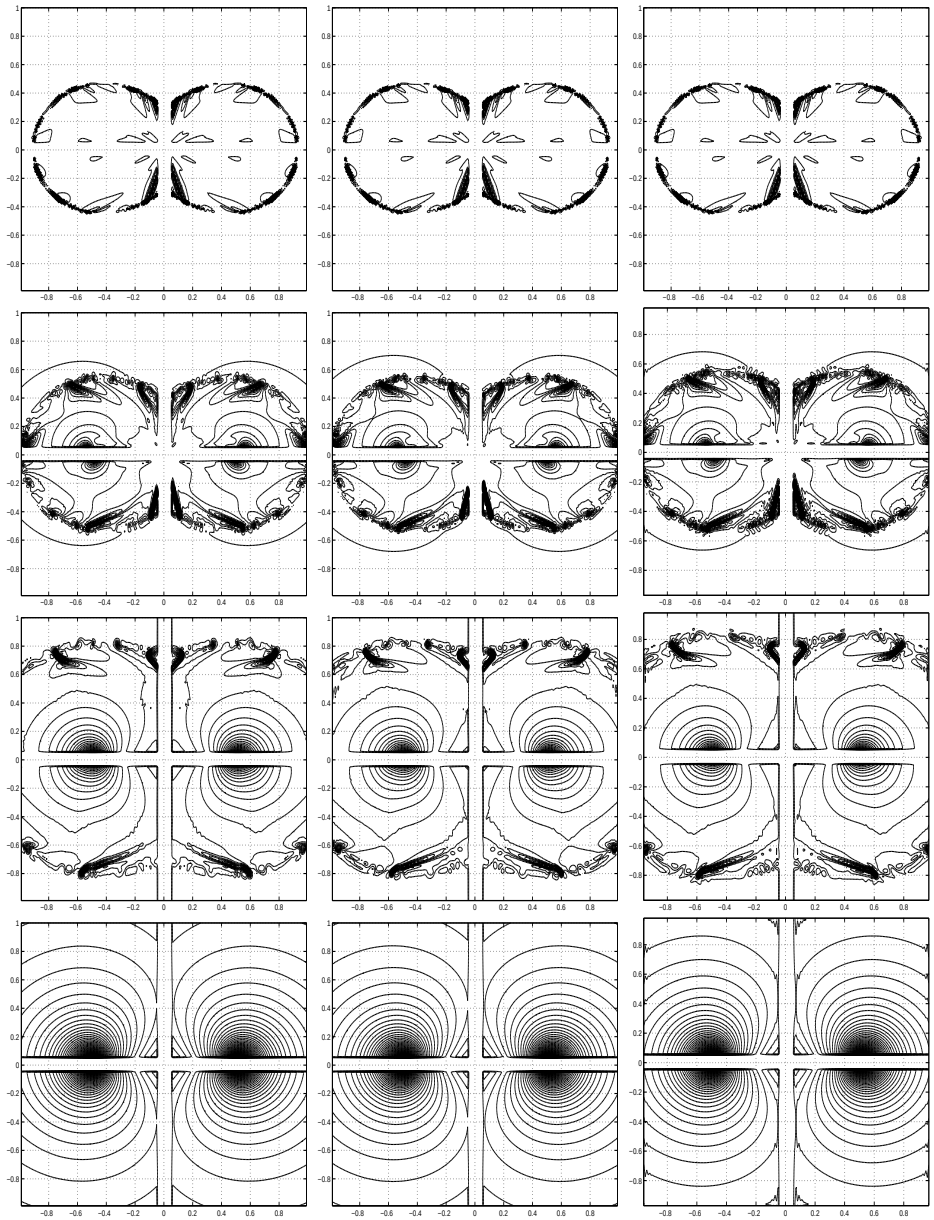

FIG. 3.7. *Curvatures at steps 0, 16, 64 and 256. Left column: WENO. Central column: WPowerENO. Right column: Weighted* Power_∞ *ENO method.*